Intracellular delivery of phosphoinositides and inositol phosphates using polyamine carriers

Shoichiro Ozaki*, Daryll B. DeWald†‡, Joseph C. Shope†, Jian Chen*, and Glenn D. Prestwich*‡§

*Department of Medicinal Chemistry, University of Utah, 30 South 2000 East, Salt Lake City, UT 84112; †Department of Biology, Utah State University, 5305 University Boulevard, Logan, UT 84322; and ‡Center for Cell Signaling, 421 Wakara Way, Suite 360, Salt Lake City, UT 84108

Edited by Bruce D. Hammock, University of California, Davis, CA, and approved August 4, 2000 (received for review May 2, 2000)

Phosphoinositide signaling regulates events in endocytosis and exocytosis, vesicular trafficking of proteins, transduction of extracellular signals, remodeling of the actin cytoskeleton, regulation of calcium flux, and apoptosis. Obtaining mechanistic insights in living cells is impeded by the membrane impermeability of these anionic lipids. We describe a carrier system for intracellular delivery of phosphoinositide polyphosphates (PIP_ns) and fluorescently labeled PIP_ns into living cells, such that intracellular localization can be directly observed. Preincubation of PIP_ns or inositol phosphates with carrier polyamines produced complexes that entered mammalian, plant, yeast, bacterial, and protozoal cells in seconds to minutes via a nonendocytic mechanism. Time-dependent transit of both PIP_ns and the carrier to specific cytosolic and nuclear compartments was readily visualized by fluorescence microscopy. Platelet-derived growth factor treatment of NIH 3T3 fibroblasts containing carrier-delivered phosphatidylinositol 4,5-bisphosphate [PtdIns(4,5)P_2]-7-nitrobenz-2-oxa-1,3-diazole resulted in the redistribution of the fluorescent signal, suggesting that fluorescent PtdIns(4,5)P_2 was a substrate for phospholipase C. We also observed a calcium flux in NIH 3T3 cells when complexes of carrier and PtdIns(4,5)P_2 or inositol 1,4,5-trisphosphate were added extracellularly. This simple intracellular delivery system allows for the efficient translocation of biologically active PIP_ns, inositol phosphates, and their fluorescent derivatives into living cells in a physiologically relevant context.

Phosphatidylinositol polyphosphates (PIP_ns) and inositol polyphosphates (IP_ns) serve as signaling molecules in numerous eukaryotic cellular processes (1–5), including tyrosine kinase growth factor and G-protein receptor signaling pathways (6, 7). PIP_ns are crucial components for endocytic, exocytic, and Golgi vesicle movement (8), and in remodeling of the actin cytoskeleton (9). Moreover, cellular phosphoinositide composition is dynamic in time and space. An ideal technique would permit visualization of both exogenously introduced and endogenously synthesized PIP_ns in membrane-associated, nuclear, and cytosolic domains.

Investigators have sought cell-permeant derivatives to deliver active PIP_ns or IP_ns intracellularly without disruption of the cell membrane. Several lipid-soluble analogs of inositol trisphosphates [Ins(1,3,4)P_3, Ins(1,4,5)P_3] and phosphoinositides [PtdIns(3,4,5)P_3] (10–12) and ''caged'' Ins(1,3,4,5)P_4, Ins(1,4,5)P_3, and $InsP_6$ have been synthesized and used in cellular studies (13). Extensive chemical synthesis (11) was required, and deprotection by light and/or esterase action was necessary to release the free IP_n or PIP_n. Because multiple protecting groups were attached to each cell-permeant molecule (13), the rate of release of the active chemical signal could not be readily controlled, and a heterogeneous mixture of potential agonists was produced.

The ability to monitor changes in cellular localization of phosphoinositides as the physiology of the cell is altered has been significantly improved by the use of green fluorescent proteins (GFPs) fused to PIP_n-specific pleckstrin homology (PH) domains (14). These chimeras are produced intracellularly and migrate to membrane sites when cells are stimulated. The GFP-PH proteins have three deficiencies that limit their generality. First, PH domains often bind to soluble IP_ns with similar affinities as for the parent PIP_n (15,16). Second, the GFP-PH constructs have not been reported to enter the nucleus or to traverse intracellular membranes. Indeed, antibodies to liposomal PtdIns(4,5)P_2 detect substantial nuclear PtdIns(4,5)P_2 (17) in mammalian cells. Finally, GFP-PH constructs are unable to affect intracellular delivery of exogenously applied PIP_ns.

To address these drawbacks, we have devised a simple procedure to deliver fluorescently labeled PIP_n and IP_n analogs into living eukaryotic cells and to monitor their subcellular localization. This approach offers an alternative to both the use of caged probes (13) and the liposome-membrane fusion method used for direct observation of activation of the protooncogene *Akt* (18) and a protein kinase C isoform (19). In this approach, a complex of the anionic PIP_n or IP_n derivative with a cationic polyamine carrier was internalized within minutes in a variety of cell types. The details of this intracellular delivery strategy and its applications in PIP_n localization, PIP_n activation of calcium flux, and PIP_n redistribution after stimulation are described herein.

Materials and Methods

Reagents. The dendrimer amine with 12 primary amines was prepared by the reduction of 12-cascade:amino(3):1-azapropylidene:(1-azabutylidene):2-propanenitrile with di-*iso*butylaluminum hydride in CH_2Cl_2. Other dendrimeric amines, including DAB-Am-32, are commercially available (Aldrich). Rhodamine B isothiocyanate (Aldrich), 7-nitrobenz-2-oxa-1,3-diazole (NBD)-X-SE, and rhodamine X isothiocyanate (XRITC) (Molecular Probes), type III-S histone from calf thymus (Sigma), and dipalmitoyl (di-C_{16}) PtdIns(4,5)P_2 and PtdIns(3,4,5)P_3 (Echelon Research Laboratories, Salt Lake City, UT) were used as supplied.

Synthesis of Fluorescent PtdInsP_n Derivatives. *sn*-2-*O*-Stearoyl PtdIns(4,5)P_2-NBD (C_{18}) and *sn*-2-*O*-palmitoyl PtdIns(3,4,5)P_3-NBD (C_{16}) were synthesized as described (20–22). A shorter chain *sn*-1-*O*-(6-aminohexanoyl)-*sn*-2-*O*-hexanoyl PtdIns(4,5)P_2 derivative was prepared analogously; reaction with NBD-X-SE was performed (21) as described to produce the PtdIns(4,5)P_2-NBD (C_6), which was characterized by proton NMR.

This paper was submitted directly (Track II) to the PNAS office.

Abbreviations: PIP_n, phosphoinositide polyphosphate; IP_n, inositol phosphate; PDGF, platelet-derived growth factor; NBD, 7-nitrobenz-2-oxa-1,3-diazole; PtdIns(4,5)P_2, phosphatidylinositol 4,5-bisphosphate; Ins(1,4,5)P_3, inositol 1,4,5-trisphosphate; GFP, green fluorescent protein; PH, pleckstrin homology; XRITC, rhodamine X isothiocyanate; MDCK, Madin-Darby canine kidney; CHO, Chinese hamster ovary; ER, endoplasmic reticulum; PLC, phospholipase C; PI3-kinase, phosphatidylinositol 3-kinase; RB, rhodamine B; Neo, neomycin.

§To whom reprint requests should be addressed. E-mail: gprestwich@deans.pharm.utah.edu.

The publication costs of this article were defrayed in part by page charge payment. This article must therefore be hereby marked "*advertisement*" in accordance with 18 U.S.C. §1734 solely to indicate this fact.

Article published online before print: *Proc. Natl. Acad. Sci. USA*, 10.1073/pnas.210197897. Article and publication date are at www.pnas.org/cgi/doi/10.1073/pnas.210197897

Ins(1,4,5)P_3-XRITC was prepared following literature procedures (23) and characterized spectroscopically.

Synthesis of Polyamine-Fluorophore Shuttles. Fluorescent derivatives of polyamines were synthesized from the amine and either the isothiocyanate or succinimidyl ester derivatives of the fluorescent reagent in 1.0 M TEAB (aqueous triethylammonium bicarbonate, pH 7.5). All compounds were purified by C_{18} HPLC, and structures were confirmed by NMR and electron spray mass spectrometry. Dendrimeric polyamines and histone were fluorescently labeled by standard protocols.

Delivery of Analogs to Cells. COS-7, Madin-Darby canine kidney (MDCK), NIH 3T3 mouse fibroblasts, and 3T3-L1 preadipocyte cells were cultured (90% DMEM, 10% calf serum) on 10-mm diameter cover slips for 12–24 h before PIP_n delivery experiments. Chinese hamster ovary (CHO) cells were cultured on cover slips in Ham's F-12 medium with 5% calf serum. Yeast (*Saccharomyces cerevisiae*) was grown in yeast extract/peptone/dextrose medium, and bacteria (*Escherichia coli*) was cultured in LB medium. *Cryptosporidium parvum* was cultured on bovine epithelial cells (24). For the PIP_n delivery experiments, dyes were added to the medium on cover slips that were mounted directly onto slides or glass plates. Images were collected without washing the dye from the medium.

Intact 1- to 2-week-old *Arabidopsis thaliana* plants grown in liquid medium were placed in glass plate wells (200 μl), fluorescent carrier-cargo complexes were added, and images of plant cells were collected 10 min later.

Microscopy. Cells were examined by using an inverted microscope (Nikon) and a Bio-Rad laser scanning confocal microscope system (MRC 1024) with LASERSHARP acquisition software. The 488-nm laser line was used for excitation of NBD-conjugated PIP_ns. The 568-nm laser line was used for neomycin (Neo)-XRITC, Neo-rhodamine B (RB), and Ins(1,4,5)P_3-XRITC. Images of animal cells were collected by using a ×60 oil immersion objective, and a ×40 objective was used for the plant cell images. No postacquisition enhancement of images was performed, except for gray-scale conversion to color using LASERSHARP software or CONFOCAL ASSISTANT software.

Organelle-Specific Stains and Endocytosis. Intracellular localization of the PIP_n and carrier fluorophore bioconjugates was determined by colocalization with commercially available organelle-specific fluorescent dyes (Molecular Probes): $DiOC_6$ [endoplasmic reticulum (ER)], BODIPY-TR ceramide (Golgi), acridine orange (nucleic acids), 4′,6-diamidino-2-phenylindole (DNA), Syto11 (nucleic acids), and FM 4–64 (plasma membrane, endosomes, and lysosomes).

Endocytosis was slowed or blocked as follows: CHO and MDCK cells were incubated in low pH medium (5.5–6.0) or at low temperature (4°C). Localization of FM 4–64 in the plasma membrane and its movement into cells was monitored via time-course optical section collection. When cells were released from either endocytic block by returning them to standard growth medium, FM 4–64 was detectably endocytosed within 5 min.

Detection of Calcium Flux in NIH 3T3 Fibroblasts. The calcium indicator dye Fluo-3 (Fluo-3 acetoxymethyl ester, Molecular Probes) was used to measure intracellular calcium concentrations by using standard curves of Fluo-3 fluorescence intensity versus calcium concentration. All calcium concentrations were measured by using confocal microscopy, glass slides, and a commercially available kit and free Fluo-3 for calibration. Intracellular pixel intensities were collected for non-nuclear portions of the cells (50 μm^2 area per collection).

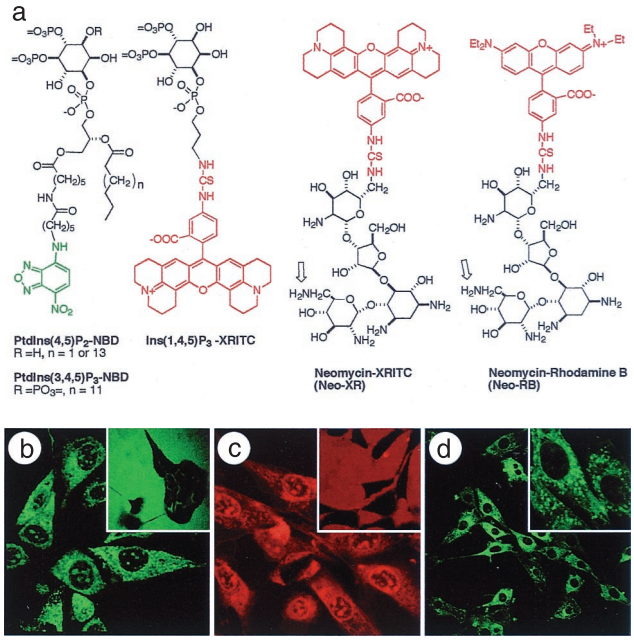

Fig. 1. Fluorescent PIP_n and IP_n analogs are rapidly delivered to cells by a polyamine carrier. (*a*) Structures of chemical probes used in this study. Left to right: fluorescent PtdIns(4,5)P_2 and PtdIns(3,4,5)P_3 analogs, fluorescent Ins(1,4,5)P_3, and two fluorescent Neo derivatives. The open arrows indicate the two primary aminomethylene (-CH_2NH_2) substituents that could be modified by the fluorophore. (*b*) NIH 3T3 mouse fibroblast cells with internalized PtdIns(4,5)P_2-NBD-histone complex; in the no-carrier control (*Inset*) the green fluorescence of PtdIns(4,5)P_2-NBD is extracellular. (*c*) Ins(1,4,5)P_3-XRITC was delivered to NIH 3T3 cells by using histone as carrier; (*Inset*) the no-carrier control. (*d*) PtdIns(3,4,5)P_3-NBD was delivered into NIH 3T3 mouse fibroblasts by using histone as carrier; (*Inset*) a higher-magnification image. Images were collected 30 min after fluorescent probe addition for no-carrier controls (*b Inset* and *c Inset*) and 5 min (*b*) or 10 min (*c* and *d*) after the complexes were added to the cells. See http: www.biology.usu.edu/pipncells/. Magnifications: *b* and *c*, ×240; *b* and *c Insets*, ×100; *d*, ×100; and *d Inset*, ×360.

Before the experiment, NIH 3T3 fibroblasts were cultured on cover slips for 12–24 h. Cover slips were mounted to a glass plate forming a well, and 0.5 μl of cell-permeant Fluo-3 acetoxymethyl ester in DMSO was added to 20 μl of medium in the well. The cells were maintained at 22°C for 15 min in the Fluo-3 solution. Then, the Fluo-3-containing medium was removed and 20 μl of fresh medium was placed in the well. Identical optical sections were collected every 30 sec for approximately 5 min to confirm that fluorescence intensity was stable, and then either an Ins(1,4,5)P_3-histone complex (concentrations 77 μM and 50 μM, respectively) or a PtdIns(4,5)P_2-histone complex (40 μM and 50 μM, respectively) was added to the cells. Optical sections then were collected every 30 sec for 20 min.

Results

The structures of the fluorescent phosphoinositides PtdIns(4,5)P_2-NBD (25) and PtdIns(3,4,5)P_3-NBD (22), the fluorescent inositol trisphosphate Ins(1,4,5)P_3-XRITC, and two fluorescent Neo carriers are shown in Fig. 1*a*. The fluorescent PIP_ns are water soluble at the concentrations used, as indicated by high-resolution NMR spectra in water. Moreover, the attachment of the fluorophore to the acyl chain does not interfere with recognition of either the IP_n head group or the attached diacylglyceryl moiety by most target proteins (20, 22, 26). All of the fluorescent and nonfluorescent carrier and PIP_n derivatives have been chemically synthesized (27) and are readily available. Each of the images presented herein used the C_6 PtdIns(4,5)P_2-NBD material, although experiments with the C_{18} analog in

CHO and MDCK cells gave identical results. Only the C_{16} analog of PtdIns(3,4,5)P_3-NBD was used in these experiments.

A number of polybasic compounds were selected as potential "charge-neutralization" species that could deliver the anionic PIP_ns in a manner analogous to intracellular delivery of oligonucleotides. Previous studies have shown that aminoglycosides interact specifically with PtdIns(4,5)P_2 (28–30) and RNA substructures (31, 32). We initially examined Neo and five other aminoglycosides as potential carrier molecules for transmembrane delivery of the fluorescent probe PtdIns(4,5)P_2-NBD (20). Certain aminoglycosides (e.g., Neo) have a relatively high affinity (K_D of $\approx$1 μM) (16) for PtdIns(4,5)P_2, similar to that of the GFP-PH fusion construct used to monitor intracellular translocation of PtdIns(4,5)P_2 (14, 33). In addition, we evaluated synthetic "spherical" dendrimeric polyamines with 12 or 32 primary amines and a polybasic nuclear protein, histone. Polyethylenimine and several amphiphilic lipofection reagents were investigated, but these were either ineffective carriers or exhibited significant cytotoxicity.

In each case, a preformed polyamine-PIP_n complex was added to the extracellular medium, and the localization of both the polyamine carrier and the cargo PIP_n or IP_n was followed by monitoring fluorescent tags using laser scanning confocal microscopy. In a preliminary survey of fluorescently modified PIP_ns and IP_ns, the efficiency of fluorophore-PIP_n delivery depended on the polyamine carrier, the PIP_n analog, and the cell type. In the absence of a polyamine carrier, the PIP_n and IP_n analogs (at concentrations of 10–30 μM) failed to enter CHO, COS-7, MDCK, 3T3-L1 preadipocytes, or NIH 3T3 mouse fibroblast cells to detectable levels within 30 min. Thus, PtdIns(4,5)P_2-NBD remains outside of NIH 3T3 cells after 30 min (Fig. 1*b Inset*). When a complex of PtdIns(4,5)P_2-NBD and histone protein was added to the medium, the PtdIns(4,5)P_2-NBD entered each of the cell types within 30 sec with saturation within 5 min (Fig. 1*b*). Similarly, a complex of Ins(1,4,5)P_3-XRITC and histone entered cells rapidly (Fig. 1*c*) with maximal accumulation at *ca.* 10 min, whereas the fluorescent inositide alone remained extracellular at 30 min (Fig. 1*c Inset*). Both PtdIns(4,5)P_2-NBD and Ins(1,4,5)P_3-XRITC possess the same P-1 phosphodiester linkage of a lipophilic moiety to the inositol-4,5-bisphosphate head group, and both derivatives show nuclear as well as cytosolic localization.

Importantly, this approach is not restricted to PtdIns(4,5)P_2 derivatives. When a complex of PtdIns(3,4,5)P_3-NBD and histone was added to NIH 3T3 fibroblasts, the PtdIns(3,4,5)P_3-NBD was detectable in cells within 2 min, with saturation at 10 min (Fig. 1*d*). No uptake into cells was observed in the absence of the histone or other suitable carrier polyamine. The intracellularly delivered PtdIns(3,4,5)P_3-NBD fluorescence localized to the plasma membrane, ER, and Golgi structures. However, unlike the PtdIns(4,5)P_2-NBD, the 3-phosphorylated lipid was excluded from the nuclei (Fig. 1*d Inset*).

These complexes could, in principle, enter by passive or active mechanisms. To test the hypothesis that cellular entry occurred by passive movement across the membrane, endocytosis was slowed (CHO cells) or blocked (MDCK cells) before addition of the carrier-PIP_n-NBD complex or a membrane-specific fluorophore as a control. Blocking or slowing endocytosis in MDCK or CHO cells had no discernible effect on the kinetics of accumulation of the polyamine carrier-PtdIns(4,5)P_2-NBD complex in these cell types. These data thus support passive movement across eukaryotic membranes. The efficiency of this process is evident from the absence of extracellular PIP_n-NBD after *ca.* 2-min incubation of cells with the PIP_n-NBD-carrier complex.

Intracellular delivery into prokaryotic cells and a spectrum of eukaryotic cell types can be achieved as illustrated in Fig. 2. Distinct cellular destinations for the carriers and PIP_n cargo molecules were observed in three mammalian cell types (Fig. 2 *a–c*). An equimolar mixture of PtdIns(4,5)P_2-NBD and Neo-RB was added to the media immediately before recording confocal images of the cells. Uptake of the PtdIns(4,5)P_2-NBD-Neo-RB complex is shown for CHO (Fig. 2*a*) and MDCK (Fig. 2*c*), whereas the complex of Neo-XRITC and PtdIns(4,5)P_2-NBD was delivered to 3T3-L1 preadipocytes (Fig. 2*b*). Fig. 2 shows the fluor localization after 10 min, but equilibrium was reached in less than 5-min incubation for most cells and complexes tested. In the three mammalian cells, the red Neo-RB (or Neo-XRITC) appeared to be concentrated in the ER and the nucleoli, consistent with its complexation to transfer RNA and ribosomal RNA subunits. The green fluorescing PtdIns(4,5)P_2-NBD can be seen in the plasma membrane and (for the mammalian cells) in intracellular patterns consistent with its presence in the ER, Golgi, the nuclear membrane, and substructures within the nucleus. The punctate staining in the nucleus is reminiscent of the mammalian cell nuclear speckles containing type I and type II PIP kinases (34) colocalized with PtdIns(4,5)P_2 (35). The dramatic colocalization (yellow color) of the PtdIns(4,5)P_2-NBD and Neo-RB in nucleoli and the ER is particularly noteworthy. The colocalization suggests that either the components migrate separately to the nucleus or that some intact complex migrates through the cytosol, across the nuclear membrane, and into the nucleoli. The kinetics of carrier-cargo interactions and an understanding of the mechanism of internalization are the subjects of ongoing research.

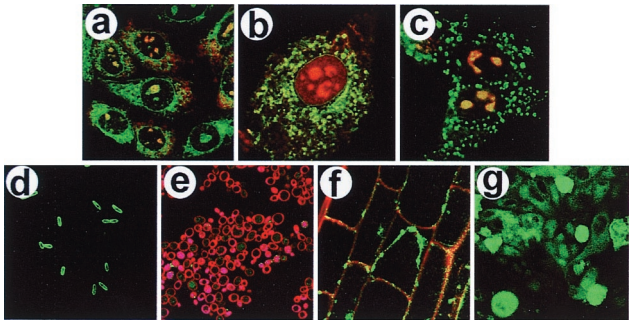

Fig. 2. Delivery of PtdIns(4,5)P_2-NBD into eukaryotic and prokaryotic cells. All images shown were recorded at 10 min after addition of the carrier-cargo complex. (*a*) The uptake of complexes of PtdIns(4,5)P_2-NBD and Neo-RB by CHO cells. (*b*) Uptake of PtdIns(4,5)P_2-NBD-Neo-XRITC complexes by a 3T3-L1 preadipocyte. (*c*) Uptake of PtdIns(4,5)P_2-NBD-Neo-RB complexes by MDCK cells. (*d*) Uptake of PtdIns(4,5)P_2-NBD (histone carrier) by *E. coli* cells. (*e*) Uptake of PtdIns(4,5)P_2-NBD (histone carrier) by *S. cerevisiae* cells. The red fluorescence in the plasma membrane is a result of FM 4–64 staining after analog delivery. (*f*) Uptake of PtdIns(4,5)P_2-NBD-Neo-RB complexes by *A. thaliana* root-tip cells. (*g*) Uptake of PtdIns(4,5)P_2-NBD (histone carrier) by *C. parvum* cells on a field of epithelial cells (background). For each image, the green fluorescence is caused by the PtdIns(4,5)P_2-NBD, the red fluorescence is emitted by either Neo-RB or Neo-XRITC (except *e*), and the yellow regions are caused by colocalization of red and green fluorophores. Magnifications: *a*, ×260; *b* and *d*, ×600; *c*, ×400; *e* and *g*, ×160; and *f*, ×480.

Intracellular delivery of PtdIns(4,5)P_2-NBD also is shown for a selection of nonmammalian cells. Thus, uptake of a histone-PtdIns(4,5)P_2-NBD into the Gram-negative bacteria *E. coli* is illustrated in Fig. 2*d*; without a carrier, no uptake was observed within 30 min. Similarly, in the budding yeast *S. cerevisiae* (Fig. 2*e*), the histone-PtdIns(4,5)P_2-NBD complex delivered the PIP_n into cells, whereas no uptake was observed with PtdIns(4,5)P_2-NBD alone. The red fluorescence in the plasma membrane results from rapid FM 4–64 staining after analog delivery. Carrier-mediated uptake is considerably slower in yeast cells than in animal or plant cells. Fig. 2*f* shows uptake of a PtdIns(4,5)P_2-NBD-Neo-RB complex into root-tip cells of the model plant (36), *A. thaliana* (Fig. 2*f*). The Neo-RB was

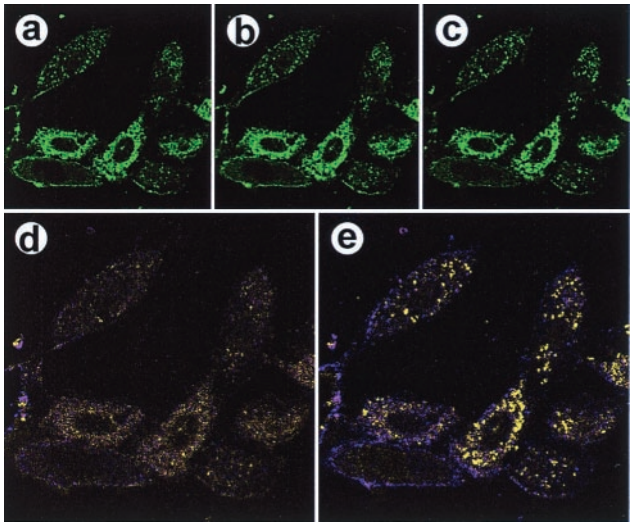

Fig. 3. PDGF stimulation of NIH 3T3 fibroblasts causes a relocalization of PtdIns(4,5)P_2-NBD. Serum-starved (3 h) NIH 3T3 cells were treated with a complex of PtdIns(4,5)P_2-NBD (10 μM) and histone (3 μM). After 10 min, cells were stimulated with 380 ng/ml PDGF; the medium was not changed subsequently. (*a*) An image before PDGF addition (t = 0), using the 488-nm laser line. The same optical section (Z-section) was collected for 20 min at 10-sec intervals. *b* and *c* were obtained at t = 3 min and 15 min, respectively. (*d*) A difference image calculated by using the t = 0 and t = 3-min data, in which fluorescence intensity corresponds to movement of the PtdIns(4,5)P_2 or its metabolic products. Thus, purple represents a decrease in fluorescence and yellow represents an increase in fluorescence in the 3-min image relative to the zero-time image. (e) A difference image comparing the 15-min data with the zero-time data. Magnifications: *a–c*, ×240; and *d* and e, ×360.

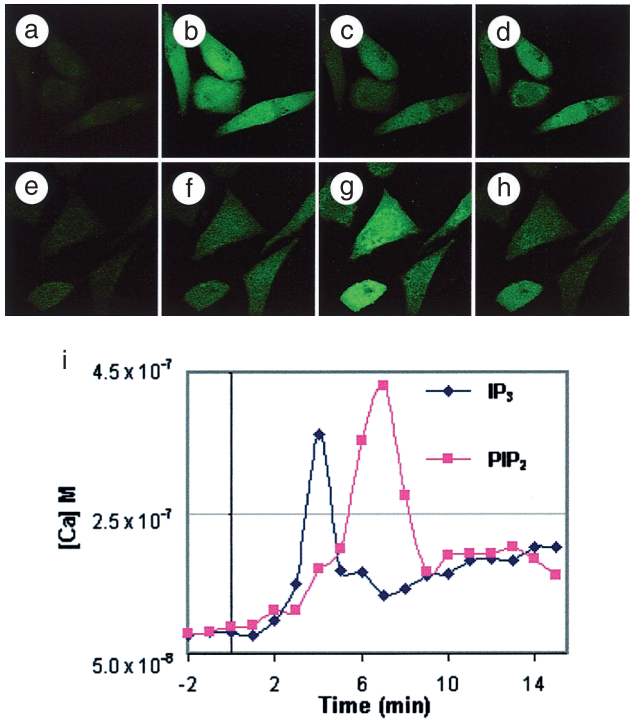

Fig. 4. Carrier-delivered Ins(1,4,5)P_3 and PtdIns(4,5)P_2 caused calcium flux in NIH 3T3 cells. Fibroblasts were loaded with Fluo-3; after 15 min, a time course of images was collected. After an additional 2 min, either an Ins(1,4,5)P_3-histone or a PtdIns(4,5)P_2-histone complex was added to the cells, and increased intracellular calcium was detected by increased green fluorescence. (*a–d*) t = 0, 4, 7, and 15 min after addition of the Ins(1,4,5)P_3-histone complex; calcium concentrations were 81 nM, 362 nM, 133 nM, and 164 nM, respectively. (*e–h*) t = 0, 4, 7, and 15 min after addition of the PtdIns(4,5)P_2-histone complex; calcium concentrations were 88 nM, 171 nM, 430 nM, and 191 nM, respectively. (*i*) A time course of subcellular pixel intensities, in min, after addition of the Ins(1,4,5)P_3-histone and PtdIns(4,5)P_2-histone complexes. The same optical section was collected for each time point by using the 488-nm excitation line (laser power 0.3%). Magnifications: *a–h*, ×240.

localized primarily in the cell wall, whereas the PtdIns(4,5)P_2-NBD appears to be sequestered in the plasma membrane. This is readily seen in the partially plasmolyzed cell at center. Finally, we observed uptake of PtdIns(4,5)P_2-NBD as the histone complex into both host bovine fallopian tube epithelial cells and the pathogenic protist *C. parvum* (Fig. 2*g*). Interestingly, the uptake into the roughly spherical *C. parvum* pathogen was more efficient than uptake into the host cells.

We next explored changes in intracellularly delivered PtdIns(4,5)P_2-NBD when the physiology of NIH 3T3 fibroblasts cells was altered. Fig. 3 shows PtdIns(4,5)P_2-NBD redistribution in platelet-derived growth factor (PDGF)-activated cells. Thus, a complex of PtdIns(4,5)P_2-NBD (10 μM) and histone (3 μM) was delivered to cells; after 10 min, cells were stimulated by treatment with 380 ng/ml PDGF, and images were obtained at 10-sec intervals for 20 min. At 0 sec, the equilibrium localization of PtdIns(4,5)P_2-NBD to the plasma membrane and to diffuse punctate and filamentous structures in the cytosol was evident (Fig. 3*a*). After 3 min, modest decreases in the plasma membrane staining and relocalization of the fluorophore in the cytosol were observed (Fig. 3*b*). At t = 15 min after addition of PDGF, nuclear and plasma membrane staining was substantially decreased, and redistribution of the fluorophore in the cytosol reached a maximum (Fig. 3*c*). In the cytosol, the NBD fluorophore relocalized in a bright punctate pattern that was consistent with ER/Golgi staining. These changes are most dramatically illustrated in the pseudocolored difference images generated from the t = 0 and 3-min data (Fig. 3*d*) and from the t = 0 and 15-min data (Fig. 3*e*). A similar set of experiments used insulin-stimulated 3T3-L1 preadipocytes (see http://biology.usu.edu/pipncells/).

The delivery of both soluble IP_n and PIP_n species into cells caused changes in intracellular calcium flux. In Fig. 4, NIH 3T3 fibroblasts were loaded with the calcium indicator, Fluo-3, which exhibits a green fluorescence proportional to calcium binding. Medium was exchanged and cells were observed until no changes in fluorescence were evident. Then, a complex of 77 μM Ins(1,4,5)P_3 and 50 μM histone was added to the medium. A time-course collection of images (Fig. 4 *a–d*) showed that cells exhibited significant increases in cytosolic calcium, with a maximum increase in Fluo-3 fluorescence in the cytosol of the treated cells occurring at 4 min. After 15 min (Fig. 4*d*) the green fluorescence of the calcium-Fluo-3 complex had decreased from a calibrated peak calcium concentration of 362 nM to a value of 164 nM. Fig. 4*i* presents quantitative data for the calcium flux in the cytosol. The efficiency of cellular uptake of carrier-IP_n complexes is substantially lower than that for carrier-PIP_n or carrier-Ins(1,4,5)P_3-XRITC complexes (Fig. 2). The PIP_n-carrier system currently favors inositides with P-1 diesters that contain lipophilic moieties.

We thus examined the ability of carrier-delivered PtdIns(4,5)P_2 to cause changes in intracellular calcium. An extracellular concentration of 40 μM of a PtdIns(4,5)P_2-histone complex was added to NIH 3T3 fibroblasts (Fig. 4 *e–h*), and calcium flux was observed. PtdIns(4,5)P_2 delivered into cells by this method can serve as a substrate for phospholipase C (PLC); the enzymatic release of Ins(1,4,5)P_3 then can produce the observed changes in intracellular calcium levels. In cells receiving carrier-delivered PtdIns(4,5)P_2, cytosolic calcium concentrations increased from 88 nM to over 430 nM at 7 min (Fig. 4*g*).

The calcium flux observed depended on PLC activity (37) because preloading of cells with the potent PLC inhibitor U73122 prevented flux in response to intracellular delivery of PtdIns(4,5)P_2 but not for intracellular delivery of Ins(1,4,5)P_3 (data not shown).

Discussion

Phosphoinositides have been implicated in diverse cellular processes that include proliferation, vesicle-mediated protein trafficking, cytoskeletal reorganization, and survival (1–3). The PIP_n kinase products PtdIns(3)P, PtdIns(3,4)P_2, PtdIns(4,5)P_2, and PtdIns(3,4,5)P_3 serve as "second messengers" (4, 5) by localizing and/or activating PIP_n-binding proteins, thereby providing a crucial link in the transmission of cellular signals. To fully understand the roles of PIP_ns, changes in their localization and metabolism and identification of specific cellular changes elicited by particular molecular species must be documented. Efforts directed toward these goals include sensitive (but laborious) biochemical quantitation with [^{3}H]inositol-loaded cells, construction and cellular expression of GFP-PH domain fusions to determine PIP_n localization (33, 38, 39), and cellular delivery of PIP_ns and IP_ns to study physiology (13, 18, 19). We have described an approach that permits intracellular delivery of PIP_ns, visualization of subcellullar PIP_n localization, and determination of PIP_n changes during specifically induced changes in cell physiology.

Three carrier molecules delivered the PtdIns(4,5)P_2-NBD and PtdIns(3,4,5)P_3-NBD into mammalian, plant, bacterial, protozoal, and yeast cells. Neither the carriers nor the PIP_ns alone showed significant intracellular uptake within 20 min. However, preincubation of the PIP_n with a dendrimeric polyamine, an aminoglycoside antibiotic, or the polybasic protein histone gave complexes that rapidly entered the cells. Internalization occurred primarily via a nonendocytic mechanism, and the time-dependent transit of both the PIP_n and the carrier to specific cytosolic and nuclear compartments could be readily visualized. Delivery of Ins(1,4,5)P_3, PtdIns(4,5)P_2, PtdIns(3,4,5)P_3, and fluorescently tagged analogs into cells also was achieved with histone. The delivery of Ins(1,4,5)P_3 and PtdIns(4,5)P_2 into NIH 3T3 fibroblasts resulted in an increased calcium flux, as visualized by Fluo-3 fluorescence.

The carrier-PIP_n complexes were preformed before addition to the extracellular medium; localization of both the polyamine carrier and the cargo PIP_n was followed by monitoring fluorescent derivatives with confocal microscopy. The efficiency of fluorophore-PIP_n or fluorophore-IP_n delivery depended on the polyamine carrier, the PIP_n or IP_n, and the cell type. For the five mammalian cell lines examined, the most rapid and efficient cellular delivery of PtdIns(4,5)P_2 and PtdIns(3,4,5)P_3 analogs was achieved by using small aminoglycoside antibiotics such as Neo and kanamycin. Dendrimeric amines were nearly as efficient as Neo, but caused cell detachment over several hours. Polyethylenimine was a partially effective carrier, but its cellular toxicity precluded its use. Other lipid transfection agents, e.g., vectamidine, did not cause intracellular delivery of PIP_n-NBD or Ins(1,4,5)P_3-XRITC. Several histones were evaluated, and each was found to be effective and essentially nontoxic as a carrier. Type III-S histone was selected for use in the majority of the intracellular delivery experiments, as it had minimal adverse effects on cell physiology.

We examined the delivery of PIP_n-NBD and other fluorescent analogs to yeast cells, an important model system for phosphoinositide-regulated vesicle-mediated protein trafficking (40), and stress responses (41). Although delivery of PIP_n into yeast was significantly slower and less efficient than into mammalian cells, PtdIns(4,5)P_2-NBD nonetheless entered the cytosol and accumulated in punctate cytosolic structures. Although the nature of these sites of PtdIns(4,5)P_2-NBD accumulation is unknown, detailed studies of the role of PIP_ns in yeast protein trafficking and environmental stress response are underway.

Delivery of PtdIns(4,5)P_2-NBD into *A. thaliana* root-tip cells also was achieved, albeit at lower efficiency than into mammalian cells. PtdIns(4,5)P_2-NBD localized in the plasma membrane of plant cells and to a lesser degree in cytosolic compartments. Combining this approach with biochemical analyses should advance our understanding of PIP_n signaling in plant cells (42).

Some bacterial and protozoan pathogens exploit mammalian host cell functions, including PIP_n signaling (43). For example, activation of host cell phosphatidylinositol 3-kinase (PI3-kinase) and cytoskeletal remodeling are responses to *Listeria monocytogenes* (44) and *C. parvum* infection (24). PtdIns(4,5)P_2-NBD was preferentially incorporated into the protozoan pathogen, *C. parvum*, relative to the cocultured bovine epithelial host cells. The PIP_n-carrier system can be used to probe the basis of invasion and alteration of host cell signaling by pathogens, leading to potential applications in the discovery of new antibiotics.

Changes in localization and metabolism of PtdIns(4,5)P_2 as a result of PDGF receptor activation was examined in serum-starved NIH 3T3 fibroblasts preloaded with a PtdIns(4,5)P_2-NBD/histone complex. PtdIns(4,5)P_2-NBD was chosen because activation of receptor tyrosine kinases and PI3-kinase could lead to conversion of PtdIns(4,5)P_2 to PtdIns(3,4,5)P_3 by PI3-kinase, or PtdIns(4,5)P_2 could act as a substrate for PLC isozymes. Both enzymatic activities are modulated by PIP_n binding in these cells. The redistribution of the NBD fluorophore in Fig. 3 suggests two possible interpretations. The PI3-kinase product PtdIns(3,4,5)P_3-NBD could be formed and move from the plasma membrane to intracellular sites. Alternatively, the diffuse perinuclear-localized fluorophore could be diacylglyceryl-NBD, derived from action of PLC on PtdIns(4,5)P_2-NBD. We favor the latter hypothesis, and chemical evidence supports this assignment. In addition, PIP_ns may recruit PLC isoforms to the plasma membrane in fibroblasts where a readily available pool of substrate exists (45, 46). Importantly, the use of PLC inhibitors (data not shown) coupled with this PIP_n delivery method further support the idea that PtdIns(4,5)P_2-NBD is acting as a substrate for PLC in the stimulated cells.

Because Ins(1,4,5)P_3 and PtdIns(4,5)P_2 have roles in calcium mobilization in mammalian cells, we examined the capacity of carrier-delivered PIP_ns and IP_ns to induce changes in cytosolic calcium concentrations (47). Indeed, both Ins(1,4,5)P_3 and PtdIns(4,5)P_2 delivery into NIH 3T3 cells resulted in cytosolic calcium mobilization. The Ins(1,4,5)P_3-induced calcium mobilization into the cytosol of fibroblasts was rapid (within 1.5 min), and calcium concentrations returned to pretreatment levels after 7 min. When PtdIns(4,5)P_2 was delivered into cells, significant calcium mobilization into the cytosol was observed with a time delay that may correspond to hydrolysis of PtdIns(4,5)P_2 to Ins(1,4,5)P_3 (47) by PLC (37). Suppression of calcium mobilization in cells preloaded with a PLC inhibitor further supported this interpretation. Taken together, the calcium mobilization results illustrate that significant and meaningful changes in cellular physiology could be manifested by the carrier-mediated intracellular delivery of Ins(1,4,5)P_3 or PtdIns(4,5)P_2.

The link between PIP_n metabolism and second-messenger calcium production is only one downstream effect on cell physiology that can be scrutinized by using this approach. First, it will be possible to study colocalization of PIP_n-binding protein PH domain/GFP fusions with specific delivered PIP_ns. Some of the important signaling molecules that are PIP_n-binding proteins include Akt/protein kinase B (38, 39, 48), phosphoinositide-dependent protein kinases (49), and ARNO (ADP-ribosylation factor nucleotide-binding-site opener) (39). Second, this approach also will prove valuable for the study of PIP_n-binding proteins in the absence of tyrosine kinase growth factor receptor activation to study specific branches of signaling pathways. Third,

delivery of PIP_n can "biochemically complement" cells expressing dominant negative PI3-kinase or other PIP_n kinase mutant proteins. Finally, delivery of PtdIns(3,4,5)P_3 could be used to rescue wortmannin-treated cells in which PI3-kinase has been chemically inactivated.

In summary, the use of the carrier-cargo system to ferry affinity-tagged or native PIP_ns into living cells provides a simple method to examine the action, localization, and metabolism of PIP_ns involved in signal transduction pathways in the context of changes in cell physiology. An important corollary is that PIP_ns and IP_ns may be used to deliver aminoglycosides, including fluorescent or synthetic analogs of antibiotics, specifically into eukaryotic cells. Given the current critical need for new antibiotic strategies, this approach allows the pursuit of molecules that could reclaim the utility of many aminoglycosides for which toxicity or resistance has reduced clinical use.

We thank Ms. W. N. Alrashid, Ms. K. Manabe, Mr. J. A. Christensen, and Mr. C. Fillmore at Utah State University, and Ms. U. Bui and Mr. M. G. Bowden at The University of Utah for their contributions in syntheses, cell culture, and microscopy. Discussions with Drs. V. H. Kang and P. O. Neilsen (University of Utah), Dr. S. McLaughlin (University of New York at Stony Brook), Dr. M. Iino (University of Tokyo), and other collaborators are gratefully acknowledged. Echelon Research Laboratories, Inc. provided di-C_{16} PIP_ns. This work was funded by grants from the National Institutes of Health, National Science Foundation, and the American Cancer Society.

1. Martin, T. F. J. (1998) *Annu. Rev. Cell Dev. Biol.* **14,** 231–264.
2. Toker, A. (1998) *Curr. Opin. Cell Biol.* **10,** 254–261.
3. Toker, A. & Cantley, L. C. (1997) *Nature (London)* **387,** 673–676.
4. Leevers, S. J., Vanhaesebroeck, B. & Waterfield, M. D. (1999) *Curr. Opin. Cell Biol.* **11,** 219–225.
5. Rameh, L. & Cantley, L. (1999) *J. Biol. Chem.* **274,** 8347–8350.
6. Stoyanov, B., Volinia, S., Hanck, T., Rubio, I., Loubtchenkov, M., Malek, D., Stoyanova, S., Vanhaesebroeck, B., Dhand, R., Nurnberg, B., *et al*. (1995) *Science* **269,** 690–693.
7. Stephens, L. R., Eguinoa, A., Erdjument-Bromage, H., Lui, M., Cooke, F., Coadwell, J., Smrcka, A. S., Thelen, M., Cadwallader, K., Tempst, P. & Hawkins, P. T. (1997) *Cell* **89,** 105–114.
8. De Camilli, P., Emr, S. D., McPherson, P. S. & Novick, P. (1996) *Science* **271,** 1533–1539.
9. Hall, A. (1998) *Science* **279,** 509–514.
10. Jiang, T., Sweeney, G., Rudolf, M. T., Klip, A., Traynor-Kaplan, A. & Tsien, R. Y. (1998) *J. Biol. Chem.* **273,** 11017–11024.
11. Li, W. H., Schultz, C., Llopis, J. & Tsien, R. Y. (1997) *Tetrahedron* **53,** 12017–12040.
12. Rudolf, M. T., Traynor-Kaplan, A. E. & Schultz, C. (1998) *BioMed. Chem. Lett.* **8,** 1857–1860.
13. Li, W. H., Llopis, J., Whitney, M., Zlokarnik, G. & Tsien, R. Y. (1998) *Nature (London)* **392,** 936–941.
14. Stauffer, T. P., Ahn, S. & Meyer, T. (1998) *Curr. Biol.* **8,** 343–346.
15. Hirose, K., Kadowaki, S., Tanabe, M., Takeshima, H. & Iino, M. (1999) *Science* **284,** 1527–1530.
16. Arbuzova, A., Martushova, K., Hangyas-Mihalyne, G., Morris, A. J., Ozaki, S., Prestwich, G. D. & McLaughlin, S. (2000) *Biochim. Biophys. Acta* **1464,** 35–48.
17. Thomas, C. L., Steel, J., Prestwich, G. D. & Schiavo, G. (1999) *Biochem. Soc. Trans.* **27,** 648–652.
18. Franke, T. F., Kaplan, D. R., Cantley, L. C. & Toker, A. (1997) *Science* **275,** 665–668.
19. Derman, M. P., Toker, A., Hartwig, J. H., Spokes, K., Falck, J. R., Chen, C. S., Cantley, L. C. & Cantley, L. G. (1997) *J. Biol. Chem.* **272,** 6465–6470.
20. Glaser, M., Wanaski, S., Buser, C. A., Boguslavsky, V., Rashidzada, W., Morris, A., Rebecchi, M., Scarlata, S. F., Runnels, L. W., Prestwich, G. D., *et al*. (1996) *J. Biol. Chem.* **271,** 26187–26193.
21. Chen, J., Profit, A. A. & Prestwich, G. D. (1996) *J. Org. Chem.* **61,** 6305–6312.
22. Tuominen, E. K. J., Holopainen, J. M., Chen, J., Prestwich, G. D., Bachiller, P. R., Kinnunen, P. K. J. & Janmey, P. A. (1999) *Eur. J. Biochem.* **263,** 85–92.
23. Dormán, G., Chen, J. & Prestwich, G. D. (1995) *Tetrahedron Lett.* **36,** 8719–8722.
24. Forney, J. R., DeWald, D. B., Yang, S., Speer, C. A. & Healey, M. C. (1999) *Infect. Immun.* **67,** 844–852.
25. Chen, J., Feng, L. & Prestwich, G. D. (1998) *J. Org. Chem.* **63,** 6511–6522.
26. Prestwich, G. D., Chaudhary, A., Chen, J., Feng, L., Mehrotra, B. & Peng, J. (1999) in *Probing Phosphoinositide Polyphosphate Binding to Proteins*, ed. Bruzik, K. S. (Am. Chem. Soc., Washington, DC), Vol. 818, pp. 24–37.
27. Prestwich, G. D. (1996) *Acc. Chem. Res.* **29,** 503–513.
28. Gabev, E., Kasianowicz, J., Abbott, T. & McLaughlin, S. (1989) *Biochim. Biophys. Acta* **979,** 105–112.
29. Schacht, J. (1978) *J. Lipid Res.* **19,** 1063–1067.
30. Tuscher, O., Lorra, C., Bouma, B., Wirtz, K. W. A. & Huttner, W. B. (1997) *FEBS Lett.* **419,** 271–275.
31. Wang, Y. & Rando, R. (1995) *Chem. Biol.* **2,** 281–290.
32. Wong, C. H., Hendrix, M., Priestley, E. S. & Greenberg, W. A. (1998) *Chem. Biol.* **5,** 397–406.
33. Varnai, P. & Balla, T. (1998) *J. Cell Biol.* **143,** 501–510.
34. Anderson, R. A., Boronenkov, I. V., Doughman, S. D., Kunz, J. & Loijens, J. C. (1999) *J. Biol. Chem.* **274,** 9907–9910.
35. Boronenkov, I., Loijens, J., Umeda, M. & Anderson, R. (1998) *Mol. Biol. Cell* **9,** 3547–3560.
36. Meinke, D. W., Cherry, J. M., Dean, C., Rounsley, S. D. & Koornneef, M. (1998) *Science* **282,** 662–667.
37. Nishizuka, Y. (1992) *Science* **258,** 607–614.
38. Gray, A., VanderKaay, J. & Downes, C. P. (1999) *Biochem. J.* **344,** 929–936.
39. Oatey, P. B., Venkateswarlu, K., Williams, A. G., Fletcher, L. M., Foulstone, E. J., Cullen, P. J. & Tavare, J. M. (1999) *Biochem. J.* **344,** 511–518.
40. Odorizzi, G., Babst, M. & Emr, S. D. (2000) *Trends Biochem. Sci.* **25,** 229–235.
41. Dove, S. K., Cooke, F. T., Douglas, M. R., Sayers, L. G., Parker, P. J. & Michell, R. H. (1997) *Nature (London)* **390,** 187–192.
42. Drobak, B. K., Dewey, R. E. & Boss, W. F. (1999) *Int. Rev. Cytol.* **189,** 95–130.
43. Finlay, B. B. & Cossart, P. (1997) *Science* **276,** 718–725.
44. Ireton, K., Payrastre, B., Chap, H., Ogawa, W., Sakaue, H., Kasuga, M. & Cossart, P. (1996) *Science* **274,** 780–782.
45. Tall, E., Dormán, G., Garcia, P., Runnels, L., Shah, S., Chen, J., Profit, A. A., Gu, Q.-M., Chaudhary, A., Prestwich, G. D. & Rebecchi, M. J. (1997) *Biochemistry* **36,** 7239–7248.
46. Bae, Y. S., Cantley, L. G., Chen, C. S., Kim, S. R., Kwon, K. S. & Rhee, S. G. (1998) *J. Biol. Chem.* **273,** 4465–4469.
47. Berridge, M. J. (1994) *Mol. Cell. Endocrinol.* **98,** 119–124.
48. Datta, S. R., Brunet, A. & Greenberg, M. E. (1999) *Genes Dev.* **13,** 2905–2927.
49. Belham, C., Wu, S. & Avruch, J. (1999) *Curr. Biol.* **9,** R93–R96.